The Role of the Joint Panel Shear Deformation in Beam-to-Column Connections Part 1: Results of the Experimental Test Program

Rahiminia, Faramarz

Namba, Hisashi

Memoirs of the Graduate Schools of Engineering and System Informatics Kobe University
No. 4, pp. 8–13, 2012. doi:10.5047/gseku.e.2012.002

The Role of the Joint Panel Shear Deformation in Beam-to-Column Connections Part 1: Results of the Experimental Test Program

Faramarz RAHIMINIA[1], Hisashi NAMBA[1]

[1]*Graduate School of Engineering, Department of Architecture*

(Received November 30, 2012; Accepted February 25, 2013; Online published March 6, 2013)

Keywords: *Joint Panel, Shear Deformation, Failure Mode, Cyclic Behavior, Rotation Capacity*

This research was performed to develop a deeper understanding in the effects of joint panel shear deformation on elasto-plastic behavior of the beam-to-column connections. Fourteen full-scale beam-to-column subassemblies were experimentally tested under cyclic loading and results are reported. Main parameters in this investigation were the joint panel strength ratio, weld joint detail, material toughness and column flange width to thickness ratio. It is shown that for each series of specimens with same failure mode of beam fracture, beam cumulative plastic rotation capacity was not strongly affected by joint panel strength ratio. Experimental test results revealed that the total cumulative plastic rotation capacity was increased by reduction of joint panel strength ratio. Even weak panel specimens with heavy flange column section, could show high amount of cumulative total plastic rotation capacity at a level comparable to other weak panel specimens.

1. Introduction

Based on observations and investigations conducted after the Northridge earthquake in the US, large joint panel shear deformation effect named as "Kinking" was recognized as one of the reasons for the brittle fractures in pre-Northridge moment resisting connections[1~4]; due to this understanding, the post-earthquake joint panel design provisions were modified to prevent excessive joint panel shear deformation[5]. In Japan, although in observations of damages of Kobe earthquake no premature brittle fracture due to the joint panel shear deformation was reported, the concerns about kinking effect were raised, as well. Kawashima et al.[6] could show the possibility of premature brittle fracture in weak panels just in specimens with very low toughness material properties. That investigation was conducted on specimens with shop welded joint detail and effect of joint panel shear deformation on field welded joint detail remained unknown. Considering all these observations and concerns in both countries, this question arises that if the role of the joint panel in beam-to-column connections has been comprehensively understood and if the current Japanese design method and practice insures the safe performance of the beam-to-column connections in future earthquakes. To answer these questions different parameters of weld joint details, column section and material toughness which might affect the joint panel behavior in two countries had to be investigated. This research performed to improve the understanding of joint panel plastification behavior and its effect on elasto-plastic behavior of steel moment connections. Fourteen full-scale beam-to-column subassemblies were experimentally tested under cycling loading and results of careful observations are reported. Main parameters in this study were the joint panel strength ratio, weld joint detail, material toughness and column flange width to thickness ratio.

2. Experimental Test Specification

2.1 Test specimens

In this study fourteen full-scale specimens with specification summarized in Table 1 were tested. Figures 1 and 2 illustrate the configuration of specimens and weld joint details, respectively. Specimens were prepared in two groups of HI as interior column and HE as exterior column using two types of weld joint details of field and shop welded joint details. Fillet welds were applied in both sides of the connection of beam web to the column flange in all specimens. In this study, one of the main test parameters was joint panel strength ratio ($_{pb}R_p$) which is given by the ratio of the joint panel to the beam full plastic strength. To have a wide range of 0.47 to 1.42 for this parameter, specimens were designed with different doubler plate thicknesses. In Table 1, $_{cb}R_p$ corresponds to the full plastic strength ratio between column and beam. In order to investigate the effect of excessive shear deformation of joint panel on heavy flange column sections, two additional weak panel specimens as HIF-W group with column flange width to thickness ratios ($_c\kappa$ in Table 1) of 7 and 5 were prepared which

Table 1 Experimental test specimen specification

Specimen ID	Members	Doubler plate	$_{pb}R_p$	$_{cb}R_p$	$_c\kappa$	Weld joint
HE05S	Beam(SN490B): H-400×200×8×13 Column(SN490B): H-300×300×10×15	-	0.51	2.09	10	Shop S-type
HE08S		PL-6	0.81			
HE10S		PL-9	0.96			
HE11S		PL-12	1.09			
HE14S		2×PL-9	1.42			
HE06F	Beam(SM490A): H-400×200×8×13 Column(SM490A): H-300×300×10×15	-	0.59	2.52		Field F-type
HE10F		PL-6	0.96			
HE13F		PL-12	1.26			
HI06F		PL-9	0.60	1.32		
HI08F		PL-16	0.80			
HI10F		PL-9&12	0.97			
HI13F		2×PL-16	1.27			
HI05FW7	Beam(SM490A): H-400×200×12×19 Column(SM490B): H-300×300×16×22	PL-12	0.48	1.10	7	
HI05FW5	Beam(SM490A): H-400×200×12×19 Column(SM490B): H-300×300×16×28		0.47	1.41	5	

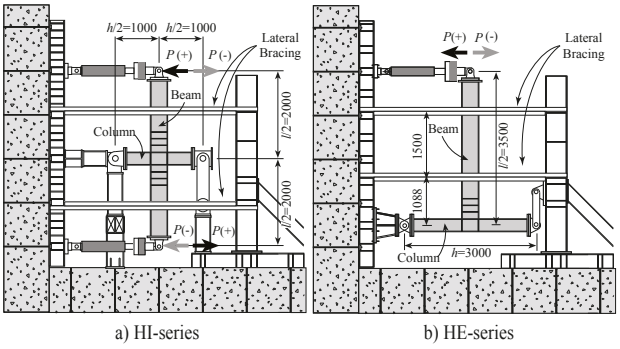

Fig. 1 Test setup

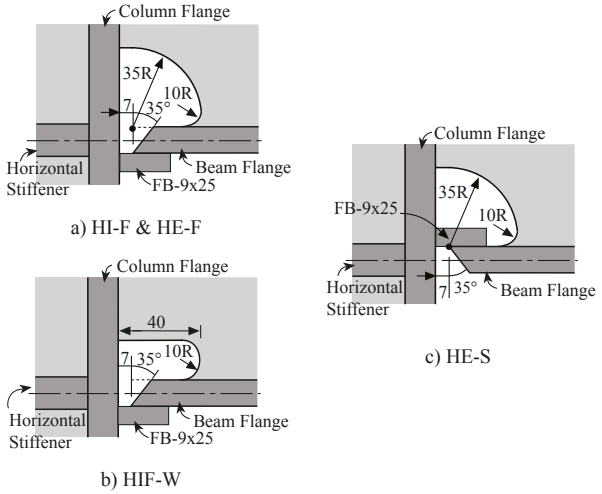

Fig. 2 Weld joint details

could be considered as representatives of heavy flange column sections commonly used in the US.

2.2 Weld joint details

Figure 2 depicts two types of field and shop welded joint details designed for beam flange to column flange connection using complete joint penetration (CJP) single bevel groove weld with steel backing bar which was left in place. In these welds steel run off tabs were used which were left in place to model more severe practice condition. The weld access hole in HI-F, HE-F and HE-S specimens was consisted of two arcs with radiuses of 35 and 10 millimetres. HIF-W specimens were specifically designed to study the effect of kinking of column and beam flanges in heavy column sections due to the excessive joint panel shear deformation, so in these specimens, different weld access hole shape was used aiming to prevent premature beam fracture at weld access hole by reducing the lack of the web section.

2.3 Material properties

The material utilized for the specimens were hot rolled sections with steel grade of SM490A (JIS G 3106) for HI-F and HE-F and SN490B (JIS G 3136) for HE-S specimens. Beam and column sections used for HIF-W specimens were fabricated from plates with steel grade of SM490A.

Actual material properties obtained by tensile coupon tests are tabulated in Table 2. One of the other parameters in this study was material toughness. Figure 3(b) plots the values of material Charpy impact test results obtained from coupon tests associated with the 'k' area (the meeting point between the web and the flange) of beam sections as shown in Figure 3 (a).

Table 2 Material properties

Specimens HE-S group		t (mm)	σ_y (N/mm^2)	σ_u (N/mm^2)	YR (σ_y/σ_u)	ε_u (%)	EL
Beam	Flange	13.0	420	569	0.74	0.17	0.42
	Web	7.90	452	579	0.78	0.19	0.35
Column	Flange	15.2	354	540	0.66	0.18	0.43
	Web	9.83	388	552	0.70	0.19	0.38
Doubler Plate	PL-6	5.73	382	551	0.69	0.26	0.37
	PL-9	9.03	384	550	0.70	0.28	0.39
	PL-12	12.6	366	526	0.70	0.25	0.42
Weld		-	384	506	0.76	0.29	0.36
HI-F and HE-F groups							
Beam	Flange	13.0	366	554	0.66	0.22	0.39
	Web	7.91	417	572	0.73	0.21	0.34
Column	Flange	14.7	377	565	0.67	0.21	0.43
	Web	10.0	398	571	0.70	0.21	0.35
Doubler Plate	PL-6	5.88	416	571	0.73	0.21	0.30
	PL-9	8.58	376	541	0.70	0.22	0.37
	PL-12	12.3	377	537	0.70	0.21	0.43
	PL-16	16.2	364	533	0.68	0.23	0.45
Weld		-	459	578	0.79	0.24	0.34
HIF-W group							
Beam	Flange	19.1	463	546	0.85	0.24	0.48
	Web	11.8	381	547	0.70	-	0.40
Column	Flange (W7)	27.7	364	547	0.67	0.16	0.48
	Flange (W5)	21.8	377	553	0.68	-	0.48
	Web	15.6	358	535	0.67	0.26	0.44
Doubler Plate	PL-12	11.8	381	547	0.70	-	0.40
Weld		-	504	612	0.82	0.12	0.53

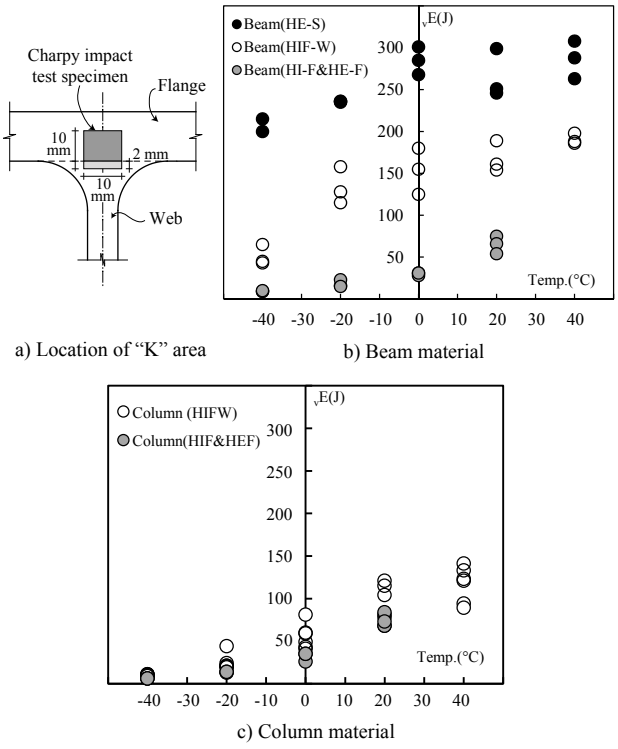

Fig. 3 Charpy impact test results

In Figure 3(b), the beam material in HE-S specimens with steel grade of SN490B with an average of 285J at 0ºC had the highest Charpy impact absorbed energy. This value was 153J

for HIF-W and the beam material in HI-F and HE-F specimens had the lowest toughness properties of 33J at 0ºC. The values of column flange material toughness are plotted in Figure 3(c). HIFW specimens were designed to investigate the effect of column flange width to thickness ratio on column flange cracking. The toughness values for column flange in this group as shown in Figure 3(c) are comparable to beam toughness values of low toughness material (HIF&HEF) in Figure 3(b). This material selection helps to prepare enough sensitive columns for cracking.

2.4 Test procedure

The cyclic reverse loading test protocol was applied consisting of 2 cycles in each 0.02 rad, 0.04 rad and the other cycles in 0.06 rad total deformation angle until the failure happened. Failure was defined as the fracture occurrence or 10% degradation from actual maximum strength obtained during the loading test.

3. Test Results

3.1 M-θ Hysteresis diagrams

M-θ_t hysteresis graphs are shown in Figure 4. In these graphs M and θ_t are the beam moment at column face and the total rotation, respectively.

From the figure, it can be observed that all weak panel specimens show a stable M-θ_t hysteresis graph. The graphs in Figures 5 and 6 show the typical cyclic behavior of beam and panel components, respectively. Beam component in balanced and strong panel specimens show bigger deformation stroke in Figure 5 compared to weak panels and in Figure 6 weak panels show bigger deformation stroke for joint panel component compared to balanced and strong panel specimens.

3.2 Observation of failure

3.2.1 Failure model

In this experimental test, typical final failure modes were beam fracture with ductile or brittle patterns and also beam local buckling as shown in Figure 7.

In weak panel specimens, after showing significant rotation capacity, beam fracture or excessive progress of ductile crack started from root of the weld access hole was observed. In both weak panel specimens with the joint panel strength ratio of 0.8, the failure mode of beam fracture was observed, regardless of material toughness. However, the failure mode in weak panel specimens with the joint panel strength ratio of less than 0.6 was found to be dependent to the material toughness. Here, no beam fracture was observed in specimens with high toughness material, even if the crack which initiated from root of the weld access hole passed through the beam flange thickness, also no significant strength reduction occurred (HE05S, HI05W5 and HI05W7). However, very weak panel specimen with low toughness material showed brittle fracture of beam flange (HE06F). Among weak panel specimens, just HI06F showed slightly different behavior. During the loading cycles of 0.06 rad, joint panel failure happened because of a later observed defect of lack of fusion in doubler plate perimeter weld.

The failure mode in strong and balanced panel specimens was strongly affected by material toughness properties. In this experimental test, specimens with high toughness material failed by local buckling and low toughness material specimens failed by fracture of beam flange due to crack initiation and progress from root of the weld access hole. Comparison of M-θ_t hysteresis graphs in Figure 4(d) for HE11S and HE14S which had high toughness material properties and failed by local buckling, also reveals that both specimens show almost same behavior until failure, but HE14S with higher panel strength ratio has failed earlier than HE11S.

3.2.2 Fracture surface

The beam fracture pattern was strongly affected by material toughness properties and ambient test temperature as reported in Table 3. Observation of crack surfaces in HE06F, HE10F, HE13F and HI08F specimens, revealed a very small area of ductile crack growth near the root of the weld access hole, followed by brittle crack through the entire section of the beam flange as illustrated in Figure 8(a). These specimens had low toughness material, which were tested at low ambient temperature (4-16 ºC). HI10F and HI13F specimens were also fabricated from low toughness material but they were tested at high ambient temperature of 20-30 ºC. In these specimens, a crack pattern with combination of brittle and ductile crack as illustrated in Figure 8(b) was observed. It was started by ductile crack growth from root of the weld access hole, followed by a stopped brittle crack progression and again ductile crack pattern. HE08S specimen with high toughness material which was tested at 15 ºC, showed a ductile crack pattern consisted of large area of ductile crack started from root of the weld access hole and edge of slit at runoff tab as illustrated in Figure 8(c).

The ambient temperature not only affected the fracture surface pattern as discussed above, but also different hysteresis behavior can be observed by comparing the hysteresis diagrams of HI10F and HI13F with HE10F and HE13F in Figure 4, respectively. While HE10F and HE13F showed lower number of loading cycles with a rapid reduction of strength at failure, HI10F and HI13F which were tested at higher ambient temperature could sustain more number of loading cycles with a gradual reduction of strength at failure.

In HIFW specimens with heavy column section, same basic failure pattern of crack progress from root of the weld access hole as the other specimens was observed.

4. Effect of joint panel

4.1 Rotation capacity

The normalized cumulative plastic rotation values for beam component, joint panel component and total deformation for experimental test results of specimens with different joint panel strength ratio are plotted in Figures 9(a), (b) and (c), respectively. The method for calculating the normalized cumulative plastic rotation is illustrated in Figure 10(a). In order to study the graphs in Figure 9, it should be considered that some specimens had different failure mode other than beam fracture. HE10S, HE11S and HE14S failed by beam local buckling, in HI06F premature failure of joint panel occurred due to a weld defect in doubler plate weld. For this specimen higher values for rotation capacity were expected. Finally, in HE05S and HI05F-W7 because of high number of loading cycles as shown in Table 3, the loading stopped before final fracture. The expected values for these specimens are shown by vertical flashes. The following discussion on effect of joint panel strength ratio on rotation capacity is presented for specimens which failed by same mode of beam fracture or excessive crack progress at weld access hole.

4.1.1 Beam behavior

The beam normalized cumulative plastic rotation (η_b) for different joint panel strength ratios ($_{pb}R_p$) are plotted in Figure 9(a) and the values are presented in Table 3. In Figure 9(a), it can be observed that for each series of HIF and HEF specimens with same failure mode of beam fracture, beam rotation capacity is almost constant. For HES specimens which failed with different aforementioned failure modes, there are not enough data to reach to the same conclusion.

It is also shown that the beam rotation capacity is strongly

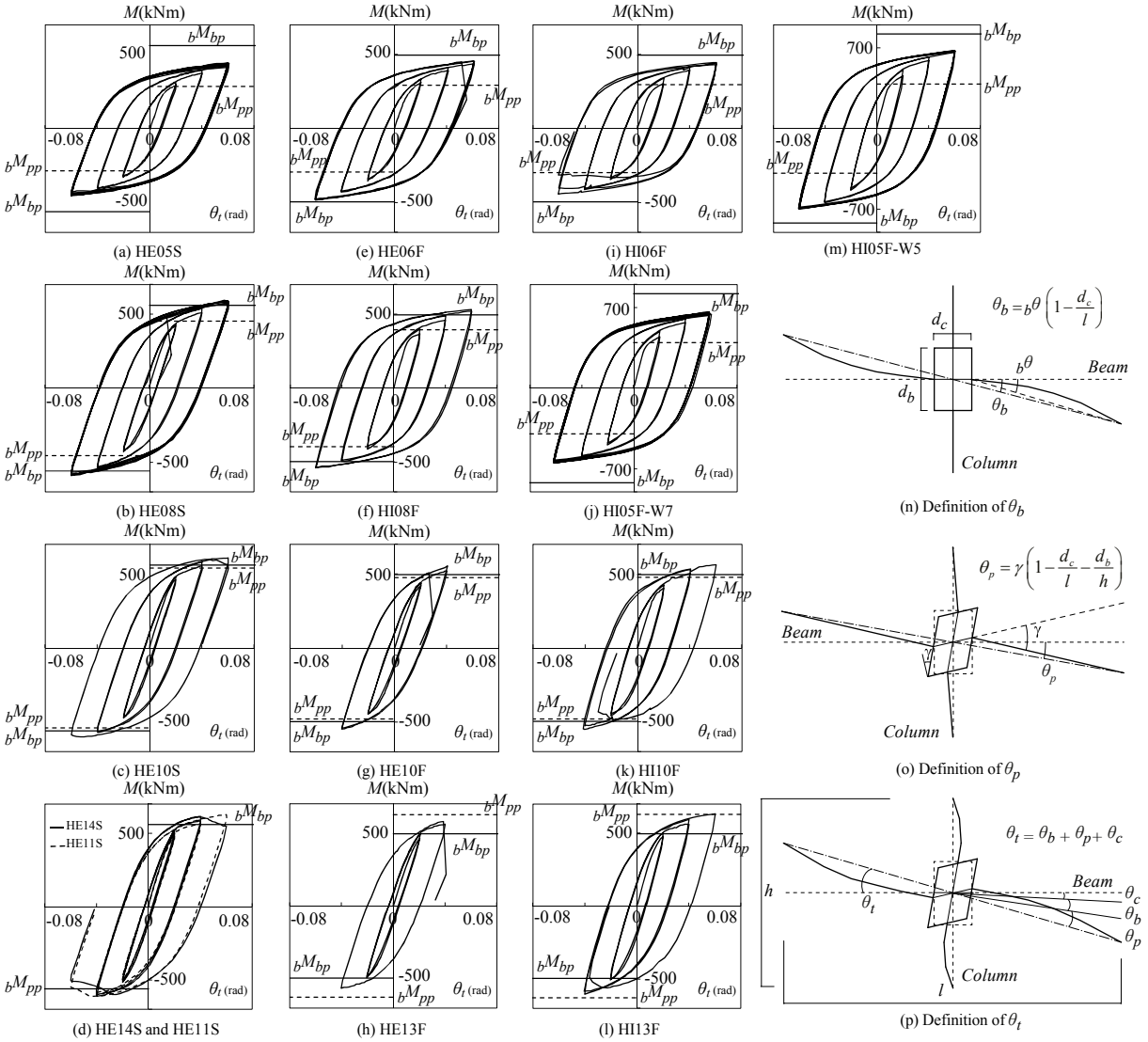

Fig. 4 M-θ_t hysteresis diagrams

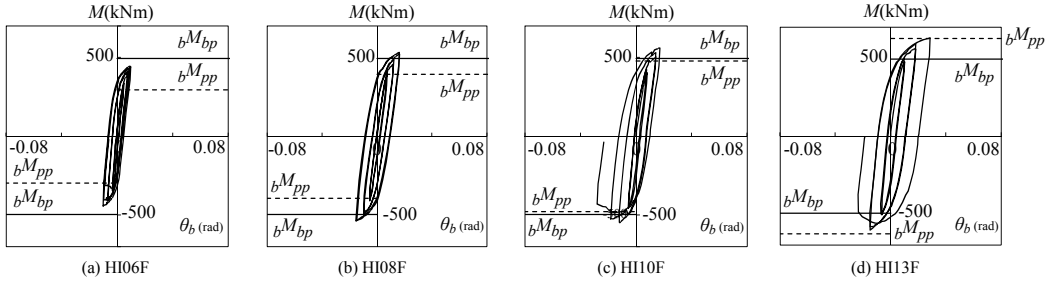

Fig. 5 M-θ_b hysteresis diagrams in HIF specimens

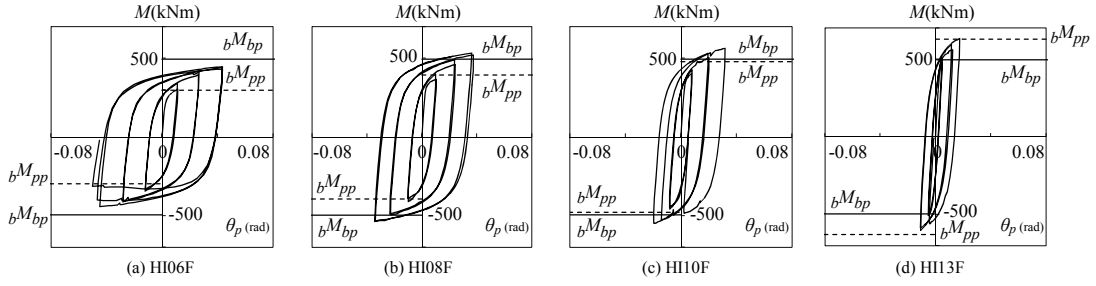

Fig. 6 M-θ_p hysteresis diagrams in HIF specimens

a) HE13F- Brittle fracture from weld access hole

b) HE14S- Beam local buckling

Fig. 7 Typical final failure modes

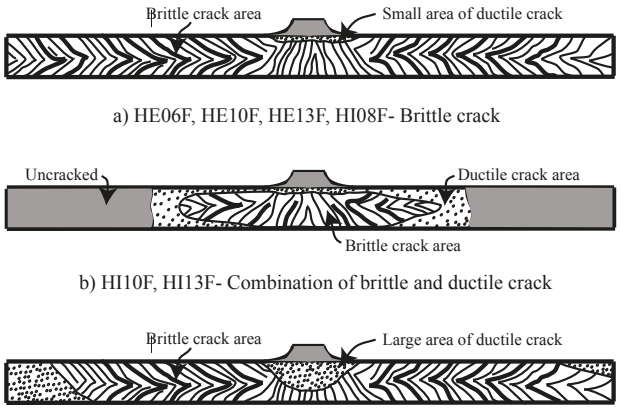

a) HE06F, HE10F, HE13F, HI08F- Brittle crack

b) HI10F, HI13F- Combination of brittle and ductile crack

c) HE08S- Ductile crack

Fig. 8 Typical fracture surfaces

affected by beam material toughness properties and ambient temperature. For the lowest material toughness and ambient temperature specimens (HE06F, HE10F and HE13F) a beam rotation capacity of almost 9 can be derived from Table 3. In specimens with same low material toughness which were tested at higher ambient temperature (HIF group), the beam rotation capacity reaches to higher values of 13~21.Here, HI06F is excluded because of difference in failure mode of joint panel failure due to weld defect. Finally, specimens with material toughness of more than 153J at 0˚C (HIFW group and HE08S) could show a beam rotation capacity of 27-39.

The reason of less effect of joint panel strength ratio to the beam rotation capacity can be explained from M-θ_b hysteresis graphs in Figure 5. Naturally, the amplitude of beam rotation in each cycle of loading is reduced by reduction of joint panel strength ratio. This reduction of cyclic amplitude can increase the number of loading cycles until final failure.

4.1.2. Joint panel behavior

The joint panel component in Figure 9(b) shows less normalized cumulative deformation in strong and balanced panel specimens compared to weak panels. This behavior can also be observed in the hysteresis diagrams of joint panel component (M-θ_p) for HIF specimens in Figure 6. The joint panel showed less deformation in balanced and strong panel specimens compared to weak panels in each loading cycle.

4.1.3 Total deformation

Normalized cumulative total deformation verses joint panel strength ratio is plotted in Figure 9(c). It can be observed that the total rotation capacity is rapidly increased by reduction of joint panel strength ratio to less than 1.0.

In Figure 9(c), the values of normalized cumulative total plastic

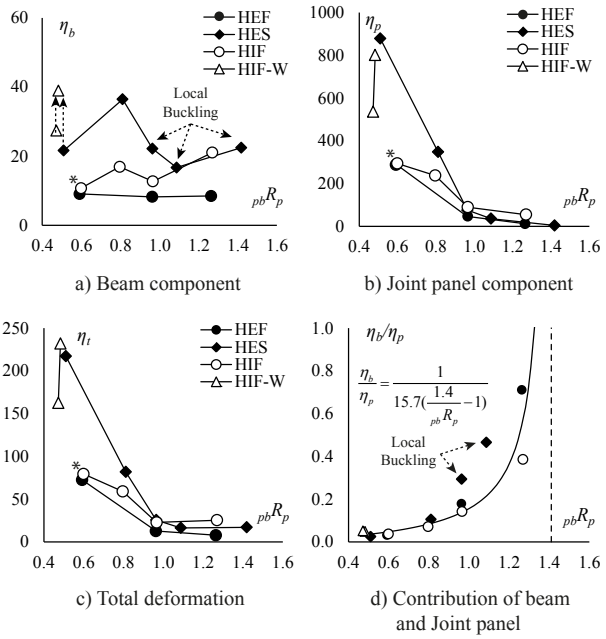

* Higher values of rotation capacity were expected for HI06F in which premature failure of joint panel occurred because of doubler plate weld defect.

Fig. 9 Contribution of components in cumulative plastic rotation

Table 3 Test results

Specimen ID	Failure θ_t(cycle)	mode[i]	$\Sigma\theta_{tpi}$ (rad)	$\Sigma\theta_{bpi}$ (rad)	$\Sigma\theta_{ppi}$ (rad)	η_t	η_b	η_p	Temp. (°C)
HE05S	0.06(+13)	JP	2.34	0.29	2.07	217	21.6	878	15 (Avg.)
HE08S	0.06(-7)	JP+SD	1.29	0.49	0.81	81.7	36.4	348	
HE10S	0.06(-2)	LB	0.47	0.30	0.18	25.5	22.1	75.4	
HE11S	0.06(-1)	LB	0.30	0.22	0.08	16.4	16.7	35.8	
HE14S	0.06(-1)	LB	0.31	0.30	0.01	17.0	22.4	3.90	
HE06F	0.06(+4)	JP+SB	0.80	0.11	0.70	72.5	9.10	290	9
HE10F	0.06(+1)	SB	0.21	0.10	0.11	12.6	8.20	46.0	4
HE13F	0.04(+2)	SB	0.13	0.10	0.03	7.70	8.50	11.9	8
HI06F	0.06(-3)	JP	0.70	0.08	0.61	79.4	10.7	294	20
HI08F	0.06(+3)	JP+SB	0.65	0.12	0.48	58.9	16.9	237	16
HI10F	0.06(-1)	SB+SD	0.29	0.09	0.18	22.7	12.7	89.5	30
HI13F	0.06(-1)	SB+SD	0.32	0.15	0.11	25.3	21.0	54.5	23
HI05F-W7	0.06(+10)	JP+SD	1.94	0.32	1.59	232	38.9	801	17
HI05F-W5	0.06(-6)	JP+SD	1.31	0.23	1.07	162	27.4	536	16

i) JP: Joint panel shear deformation, SB: Brittle fracture from scallop (weld access hole), SD: Ductile fracture from scallop, LB: Beam local buckling

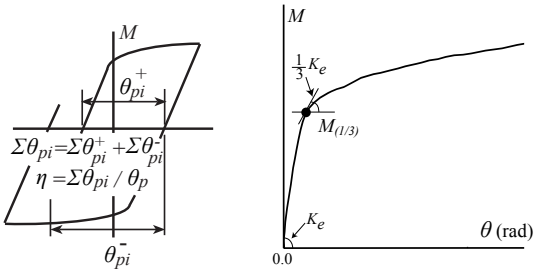

a) Cumulative plastic rotation

b) Actual plastic strength

Fig. 10 Definitions

deformation for weak panel specimens with low material toughness (HE06F, HI06F and HI08F) exceed 50, and also as shown in Table 3, all these specimens could sustain enough cycles of loading at 0.06 rad. Therefore, these weak panel specimens with low toughness material (SM-series) could show a satisfactory performance for seismic applications.

HIFW specimens with weak panel, low toughness and heavy column flanges with moderate toughness for beam showed comparable behavior as the other high toughness weak panel specimen (HE05S). Here, width to thickness ratio of column flange showed to have no effect on the rotation capacity. In Figure 9(d), the ratios of the beam to joint panel normalized cumulative plastic deformations for all specimens with different joint panel strength ratios are plotted. As it is illustrated in the figure, this ratio can be well estimated as a function of joint panel strength ratio.

In this graph two specimens of HE10S and HE11S which are illustrated by solid diamonds, show nonconformity to the empirical estimation due to the fact that these specimens had different failure pattern of beam flange local buckling. The empirical estimation shows that the joint panel contribution is increased by reduction in the joint panel strength ratio.

4.2 Strength

The skeleton curves obtained from M-θ_t hysteresis diagrams are plotted in Figures 11(a), (b) and (c) in which the total moments corresponding to one-third stiffness reduction are shown by hollow circles. The method for plotting the skeleton curves is illustrated in Figure 11(d) and the one-third stiffness method is shown in Figure 10(b). In Figures 12(a) and (b), the normalized values of total moment corresponding to one-third stiffness reduction ($M_{t(1/3)}$) and maximum moment (M_{max}) to beam theoretical plastic capacity ($_bM_{bp}$) are plotted, respectively for different joint panel strength ratios. In Figure 12(a), the ratio of the total moment corresponding to one-third stiffness reduction to the beam theoretical plastic capacity is decreased linearly by reducing of joint panel strength ratio. In this graph, the plotted test results are located lower than the dash line which is corresponded to the calculated theoretical strength, except for a strong panel specimen.

In Figure 12(b) compared to Figure 12(a) the effect of joint panel strength ratio on the ratio of the maximum moment to the beam theoretical plastic capacity is very limited.

Among weak panel specimens in this figure, just for the specimen with joint panel strength ratio of 0.8, the maximum moment could reach to the beam theoretical plastic capacity.

5. Conclusions

This experimental study was performed on fourteen full scale subassemblies to understand the effect of joint panel shear deformation on elasto-plastic behavior of beam-to-column connections. The following conclusions are made:

- In each series of specimens with same failure mode of beam fracture, the beam cumulative rotation capacity was not strongly affected by joint panel strength ratio.
- The total rotation capacity was increased by reduction in the joint panel strength ratio and higher total rotation capacity was shown by specimens with higher material toughness properties although the total rotation capacity obtained by weak panel specimens with low toughness material was still satisfactory for seismic applications.
- A combination of material toughness properties and ambient test temperature, governed the fracture pattern and crack surface which started from the root of the weld access hole.
- The maximum total strength was decreased by reduction in joint panel strength ratio but weak panel specimens with joint panel strength ratio of 0.8 could show a maximum strength higher than the beam plastic capacity.

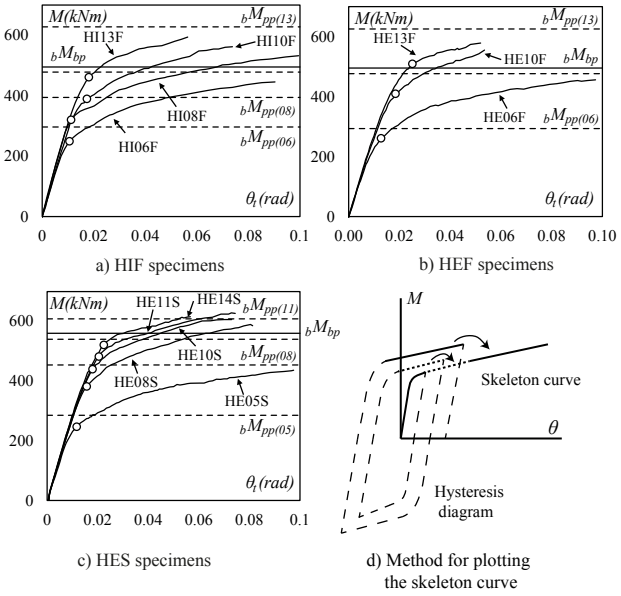

Fig. 11 M-θ_t Skeleton curves

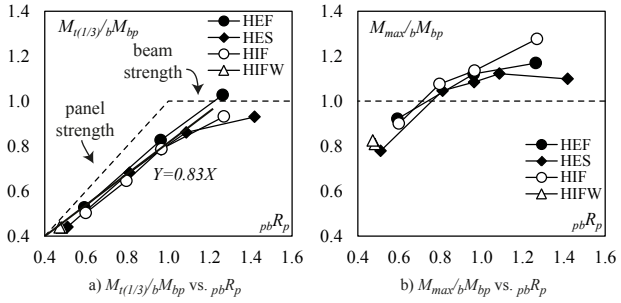

Fig. 12 Maximum and total yield moments

Acknowledgement

The research described in this paper was supported by grants from Ministry of Education of Japan under the project No: 21560591, which is truly acknowledged.

References

1) FEMA 350; "Recommended seismic design criteria for new steel moment-frame buildings, State of the art report on connection performance," Federal Emergency Management Agency, Washington D.C. (2000)
2) FEMA 355D; "State of the art report on connection performance," Federal Emergency Management Agency, Rep. FEMA 355D. Washington D.C. (2001)
3) El-Tawil S.; "Panel zone yielding in steel moment connections," *Eng. J. AISC*, 3qtr00, 120-131 (2000)
4) Ricles J.M., J.W. Fisher, L.W. Lu and E.J. Kaufmann; "Development of improved welded moment connections for earthquake-resistant design," *J. Const. Steel R.*, 58, 565-604 (2002)
5) AISC Committee on Specifications; "Seismic provisions for Structural Steel Buildings," ANSI/AISC 341-10 (2010)
6) Kawashima T., M. Tabuchi and T. Tanaka; "Effects of shear behaviour of column-to-beam joint panel on beam elastic-plastic behaviour," AIJ, 2050, 213-216 (2000)